MULTI-METHOD DIAGNOSIS OF CRANKSHAFT POSITION SENSOR INTERFERENCE IN A THREE-CYLINDER ENGINE FOR AUTOMOTIVE VOCATIONAL TRAINING

Arya Vallenra Melupite[1*], Tammy Tinny Veissy Pangow[2], Paul Maarthen Rumangit[3]
[1,2,3]Politeknik Negeri Manado, Indonesia
*Corresponding Author: melupitearya01@gmail.com

ABSTRACT
Crankshaft Position (CKP) sensor interference can disrupt crankshaft synchronization and contribute to asymmetric ignition failure in Electronic Control Unit (ECU)-based engine management systems. This study analyzed CKP parameter deviations in a single Daihatsu Xenia 1.0 non-VVT-i vehicle equipped with an EJ-DE three-cylinder engine and examined a low-cost, multi-method diagnostic sequence for workshop and automotive vocational-training contexts. The study was designed as a single-vehicle diagnostic experimental case comparing operational reference specifications, the faulty condition, and the post-repair condition. Data were obtained through OBD-II scanning, cold and hot coil-resistance measurements, reported signal-amplitude and frequency measurements, and CKP air-gap inspection. In the faulty condition, DTCs P0335 and P0336 were recorded, idle speed fluctuated at 650-710 rpm, STFT reached +18-22%, coil resistance increased to 3,180 Ω at 20°C and 3,740 Ω at 80°C, the reported signal amplitude decreased to 0.3-0.5 Vpp, frequency fell to 410 Hz, and the air gap was recorded at 0.58 mm. After sensor replacement and air-gap adjustment to 0.30 mm, the measured parameters returned to the operational reference ranges. These findings corroborate a diagnosis involving concurrent electrical and mechanical abnormalities in this specific vehicle, but the combined repair does not isolate the independent effect of each abnormality. The diagnostic sequence may support evidence-based troubleshooting practice in automotive vocational education; its instructional effectiveness and transferability require further validation.

Keywords: Automotive Diagnostics, Automotive Vocational Training, Crankshaft Position Sensor, Ignition Misfire, Sensor Fault Diagnosis

INTRODUCTION

Modern electronic fuel-injection systems depend on an Engine Management System (EMS) in which the Electronic Control Unit (ECU) continuously processes sensor inputs and issues actuator commands for fuel injection, ignition, and related engine functions. Automotive diagnostic research increasingly exploits ECU and onboard data because these signals provide a direct view of operating states and control responses (Canal et al., 2024; Mohammadpour et al., 2012). Within this architecture, the Crankshaft Position (CKP) sensor supplies a primary crank-angle and rotational-speed reference. Position-sensor research confirms the importance of reliable crankshaft position information for synchronization and engine-control functions (Petrov et al., 2020). In passive magnetic pickup configurations, changes in magnetic coupling at the rotating reluctor generate an electrical signal whose usable amplitude and timing depend on sensor condition, rotational speed, and sensor-to-reluctor geometry.

CKP signal integrity is particularly important when investigating irregular ignition because engine-control strategies infer combustion timing and cylinder behavior from crankshaft-related information. Classic and later misfire-detection studies show that crankshaft angular-speed behavior can carry diagnostic information without requiring a dedicated in-cylinder sensor (Kiencke, 1999). At the same time, sensor faults may be difficult to separate from system-level faults when evidence is taken from only one signal. Multi-information fusion, model-based estimation, and broader sensor-fault diagnosis research therefore emphasize corroboration across multiple information sources and explicit treatment of uncertainty (Hu et al., 2018; Huang et al., 2023; Trapani & Longo, 2023).

The case examined in this study involved one Daihatsu Xenia 1.0 non-VVT-i with an EJ-DE three-cylinder engine and a Denso ECU. The vehicle presented heavy misfire symptoms. Preliminary inspection indicated that the ignition behavior was asymmetric: cylinder 1 retained a consistent trigger while cylinders 2 and 3 did not. This pattern motivated an upstream diagnostic investigation of the CKP signal path rather than an assumption that two independent ignition coils had failed simultaneously.

The misfire-diagnosis literature provides several complementary methodological traditions. Crankshaft-speed, observer-based, residual-generation, and energy-model approaches have been used to detect or localize combustion irregularities from rotational dynamics (Geveci et al., 2005; Ilkivová et al., 2002; Jung et al., 2015; Macián et al., 2006; Osburn et al., 2006; Tinaut et al., 2007; Wang & Chu, 2005). Vibration and vibro-acoustic approaches have also shown that engine-block or crankshaft responses can discriminate misfire and related faults (Chang et al., 2002; Delvecchio et al., 2018; Devasenapati et al., 2010; Firmino et al., 2021; Hmida et al., 2021; Jafarian et al., 2018; Sharma et al., 2014). More recent work extends diagnosis through neural networks, simulation-assisted classification, torque estimation, multi-domain deep learning, and broader automotive predictive-maintenance frameworks (Chen & Randall, 2015; Liu et al., 2013; Qin et al., 2021; Theissler et al., 2021; Wang et al., 2020; Zheng et al., 2019). These advanced methods are valuable for automated, subtle, or predictive diagnosis, but they typically depend on additional sensing, curated datasets, modeling effort, or computational infrastructure.

The research gap addressed here is therefore not a new physical principle of CKP sensing or a claim that conventional diagnosis supersedes advanced analytics. Rather, it concerns the integrated use of accessible workshop measurements as mutually corroborating evidence in a partial and asymmetric ignition-failure case. Existing reviews describe a broad spectrum of automotive fault-diagnosis methods and emphasize the value of combining complementary evidence (Delvecchio et al., 2018; Mohammadpour et al., 2012; Theissler et al., 2021). The novelty of the present study is application- and integration-oriented: OBD-II observations, coil resistance, reported signal amplitude and frequency, and mechanical air-gap inspection are sequenced under faulty and post-repair conditions within one explicitly bounded EJ-DE case.

Accordingly, this study aimed to analyze the relationship between CKP parameter deviations and the observed ignition failure in cylinders 2 and 3 of the tested EJ-DE engine and to evaluate whether four complementary conventional diagnostic methods could provide a coherent, cross-verified diagnosis. A secondary aim was to articulate how the diagnostic sequence could be used as a competency-oriented troubleshooting framework in automotive vocational training without claiming that learner outcomes or instructional effectiveness were empirically tested in this study.

METHOD

This study used a single-vehicle diagnostic experimental case design. The sole test object was one Daihatsu Xenia 1.0 non-VVT-i equipped with an EJ-DE three-cylinder engine, a Denso ECU, and a passive magnetic pickup CKP sensor. Testing was conducted at MotoXpress Otomoto Autocare, Wanea, Manado. The design compared three states: operational reference specifications used in the diagnostic procedure, the observed faulty condition, and the post-repair condition. Because the study involved one vehicle, inference is limited to the tested configuration and to the diagnostic logic demonstrated by this case; it is not a population-level validation study.

The diagnostic sequence is summarized in Figure 1. The four measurement routes were deliberately used as complementary checks: OBD-II scanning identified ECU-level symptoms; resistance testing evaluated the sensor coil and circuit continuity; signal-amplitude and frequency measurements assessed the electrical output under operating conditions; and air-gap inspection assessed a mechanical factor capable of attenuating an inductive sensor signal. Post-repair remeasurement was then used to determine whether the observed parameters returned to the operational reference ranges.

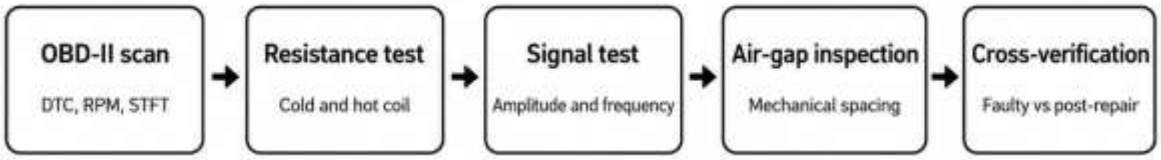

Figure 1. Multi-method diagnostic workflow used in the single-vehicle CKP case

Operationally, the procedure followed a hypothesis-testing sequence rather than four isolated measurements. A CKP-related DTC or abnormal live-data pattern was treated as an initial indication rather than a final diagnosis. Resistance testing was then used to determine whether the sensor coil or its immediate circuit showed an electrical abnormality. Signal-amplitude and frequency measurements were used to determine whether the recorded sensor output was consistent with the operational reference condition at several engine speeds. Finally, air-gap inspection assessed whether sensor-to-reluctor spacing could plausibly contribute to attenuation of the inductive signal. The post-repair retest repeated the same core observations so that the diagnosis was judged from convergence across electrical, mechanical, and ECU-level evidence rather than from a single parameter.

Operational Reference Specifications

Table 1. Reported CKP and engine reference parameters

Parameter	Nominal/Specification	Reference Range	Unit	Condition/Note
Engine type	EJ-DE	-	-	989 cc; 3 inline cylinders; non-VVT-i
Maximum power	57/5,200	-	PS/rpm	Reported vehicle specification
Maximum torque	90/3,600	-	N·m/rpm	Reported vehicle specification
Idle speed	800	800–1,000	rpm	No load
ECU	Denso	-	-	OBD-II compliant
CKP sensor	Magnetic pickup	-	-	Mounted adjacent to crankshaft reluctor
Coil resistance at 20°C	2,100	1,850–2,500	Ω	Cold condition
Coil resistance at 80°C	2,600	2,250–3,000	Ω	Hot condition
Air gap	0.30	0.20–0.40	mm	Sensor-to-reluctor spacing
Sensor-connector bias/reference reading	5.0	4.8–5.2	VDC	Ignition ON
CKP output frequency at idle	480	450–510	Hz	800–1,000 rpm

Parameter	Nominal/Specification	Reference Range	Unit	Condition/Note
CKP output frequency at higher speed	1,130–1,410	Reported range	Hz	2,000–2,500 rpm

The numerical ranges in Table 1 are the operational reference specifications reported in the original diagnostic record. The manuscript source did not provide a service-manual or other authoritative citation for these thresholds; therefore, they are treated here as diagnostic reference values used in the workshop procedure rather than independently verified manufacturer specifications.

OBD-II Scanning

The OBD-II examination used a Vgate iCar II (ELM327-type adapter) paired with the OBD Fusion application on a smartphone. The engine was warmed at idle for approximately 5 minutes, with the transmission in neutral and the parking brake engaged. The procedure read generic CKP-related DTCs, including P0335, P0336, and P0339, together with live idle-speed and Short-Term Fuel Trim (STFT) data. Freeze-frame data were inspected when available, and stored DTCs could be cleared before a retest to determine whether the fault reappeared. Each reading stage was repeated three times. The adapter was selected because it could access the generic OBD-II data required for this case; no direct comparison with a professional-grade scan tool was conducted, so equivalence in measurement accuracy is not claimed.

During OBD-II testing, the vehicle remained stationary, the transmission was kept in neutral, and the parking brake was applied. When DTCs were cleared, the engine was retested to determine whether the codes reappeared under the same general operating condition. The diagnostic application was also used to inspect freeze-frame information when available. These procedural controls were intended to make the faulty and post-repair observations comparable, although the source record does not provide a separate log of each repeated scan.

Resistance Measurement

Sensor-coil resistance was measured with a digital multimeter after the CKP connector was disconnected from the ECU harness. Cold measurements were taken at approximately 20°C, with ambient temperature checked using a digital thermometer. Hot measurements were taken after the engine had idled for approximately 10–15 minutes and the sensor body was near 80°C, as checked with an infrared thermometer before shutdown. The reference ranges used were 1,850–2,500 Ω at 20°C and 2,250–3,000 Ω at 80°C. Ground-path resistance and connector/cable resistance were also checked against the operational thresholds of <0.2 Ω and <0.1 Ω, respectively. Each resistance measurement was repeated three times. The make/model, measurement range, and manufacturer-rated accuracy of the multimeter were not documented in the source record; accordingly, those instrument-traceability details cannot be reported without speculation.

Signal-Amplitude and Frequency Measurement

Voltage and frequency checks were conducted with a digital multimeter while standard workshop safety precautions were maintained. Supply voltage was checked at the ACC/ignition position and during cranking. The sensor-connector bias/reference reading was checked against 5.0 VDC ± 0.2 V. Signal amplitude and frequency were recorded at idle and at selected engine speeds of approximately 900, 1,500, 2,000, and 2,500 rpm, with three repeated readings at each point. The source record expresses the signal-amplitude values as Vpp; however, no oscilloscope or waveform-capable acquisition instrument is documented. Therefore, the revised manuscript reports the recorded amplitude and frequency values but does not interpret waveform shape, pulse morphology, or missing-pulse patterns. Claims such as “distorted waveform” and “consistent sinusoidal waveform” have been removed because they are not supported by the documented measurement equipment.

For the cranking check, the ignition and fuel-injection functions were temporarily disabled as a workshop safety measure, and two operators were used: one operated the ignition key while the other observed the measuring instrument. Supply-line voltage drop and ground offset were also checked against the 0.2 V operational limit reported in the source method. These checks helped separate a CKP-specific abnormality from a general low-voltage condition during starting.

Air-Gap Measurement

The CKP air gap was inspected with a digital caliper reported to have 0.01 mm resolution. With the engine OFF, the sensor tip was checked for adhered metallic debris, the sensor mounting was inspected, and the gap between the sensor tip and reluctor teeth was measured at four pulley positions separated by approximately 90°. The operational reference range used in the diagnosis was 0.20–0.40 mm, with 0.30 mm as the nominal value. The source record reports 0.58 mm as the abnormal air-gap value but does not preserve the four position-specific readings; consequently, 0.58 mm is presented as the recorded representative abnormal value rather than as a reconstructed mean or maximum. The make/model and manufacturer-rated accuracy of the caliper were not documented.

Data Analysis, Reproducibility, and Ethical Scope

Analysis was descriptive and comparative. Faulty-condition values were compared with the operational reference ranges and then with the post-repair measurements. No inferential statistical test was appropriate because the study involved a single vehicle rather than a sample of independent vehicles. Although the procedure states that several readings were repeated three times, the source dataset available for this revision retains only representative values or operating ranges rather than the individual replicate observations; mean ± standard deviation therefore cannot be reconstructed. No human-participant outcomes or identifiable personal data were collected. The source record does not document a separate institutional ethics review, written vehicle-access authorization, or the replacement sensor part number, and no such information is claimed in this revision.

RESULTS AND DISCUSSION

The tested vehicle exhibited engine vibration, reduced performance, and misfire symptoms before repair. Table 2 consolidates the diagnostic evidence using consistent labels for the reference specification, faulty condition, and post-repair condition. The revised table deliberately excludes waveform descriptors because the documented method did not include an oscilloscope.

Table 2. CKP diagnostic results before and after repair

Test Parameter	Reference Specification Used in Diagnosis	Faulty Condition	Post-repair Condition
OBD-II DTC	No active CKP DTC	P0335; P0336	No active code after clearing and retest
Idle speed	800–1,000 rpm	650–710 rpm; fluctuating	910 rpm
STFT/live-data status	Stable operational condition	+18–22%	±5–8%

Test Parameter	Reference Specification Used in Diagnosis	Faulty Condition	Post-repair Condition
Coil resistance, 20°C	1,850–2,500 Ω	3,180 Ω	2,140 Ω
Coil resistance, 80°C	2,250–3,000 Ω	3,740 Ω	2,650 Ω
Sensor-connector bias/reference	4.8–5.2 VDC	4.96 VDC	5.01 VDC
Supply voltage, ACC	11.5–12.5 V	12 V	12 V
Supply voltage, cranking	≥10.5 V	11 V	11 V
Reported CKP signal amplitude, idle	1.0–1.5 Vpp	0.3–0.5 Vpp	1.1–1.4 Vpp
Air gap	0.20–0.40 mm	0.58 mm	0.30 mm
CKP output frequency, idle	450–510 Hz	410 Hz	485 Hz
CKP output frequency, 2,000–2,500 rpm	1,130–1,410 Hz	980–1,240 Hz	1,150–1,390 Hz

The protocol specified repeated readings, but the retained report does not provide the individual replicate values. Consequently, Table 2 reports the values and ranges available in the study record rather than means, standard deviations, or confidence intervals. This limitation should be considered when judging measurement stability.

OBD-II Findings

In the faulty condition, the scanner recorded P0335 (CKP Sensor “A” Circuit Malfunction) and P0336 (CKP Sensor “A” Range/Performance). P0339 was included in the diagnostic check but was not recorded in this case. The revised interpretation does not infer a specific pulse-loss mechanism from the absence of P0339 because the documented measurements do not provide waveform-level evidence. The idle speed of 650–710 rpm was below the 800–1,000 rpm operational reference range, and STFT increased to +18–22%, indicating substantial ECU fuel-trim compensation during the fault condition. After repair, idle speed returned to 910 rpm, STFT decreased to ±5–8%, and no active CKP DTC was recorded after clearing and retesting. These changes are consistent with recovery of a more stable engine-management input condition.

Resistance and Circuit Findings

The CKP coil resistance was 3,180 Ω at approximately 20°C and 3,740 Ω at approximately 80°C, both above the operational reference ranges used in the procedure. Elevated resistance under both temperature conditions is consistent with deterioration or partial discontinuity in the sensor coil, but the internal winding was not physically opened or microscopically inspected; therefore, a specific internal failure mechanism cannot be stated as directly observed. Ground-path resistance was reported at 0.1 Ω and connector resistance at 0 Ω, both within the operational thresholds described in the method. Following sensor replacement, resistance values decreased to 2,140 Ω at 20°C and 2,650 Ω at 80°C. The before–after pattern corroborates the interpretation that the original CKP sensor contributed materially to the fault condition.

Signal and Supply Findings

The sensor-connector bias/reference reading remained stable at 4.96 VDC in the faulty condition and 5.01 VDC after repair. Vehicle supply voltage was also stable at 12 V in the ACC condition and 11 V during cranking. These observations reduce the likelihood that the reported fault pattern was primarily caused by a general vehicle power-supply problem. By contrast, the recorded CKP signal amplitude at idle decreased to 0.3–0.5 Vpp in the faulty condition compared with the operational reference of 1.0–1.5 Vpp, while idle-frequency measurement fell to 410 Hz compared with the 450–510 Hz reference range. After repair, the reported amplitude increased to 1.1–1.4 Vpp and frequency to 485 Hz. Because no waveform-capable instrument is documented, these findings are interpreted only as changes in the reported amplitude and frequency measurements, not as evidence of a particular waveform shape or missing-pulse sequence.

Air-Gap Findings

The abnormal air gap was recorded at 0.58 mm, exceeding the 0.20–0.40 mm operational reference range. For an inductive magnetic pickup sensor, increasing the sensor-to-reluctor distance can reduce magnetic coupling and therefore attenuate the electrical signal available to the ECU. This mechanical observation is directionally consistent with the reduced signal-amplitude and frequency readings observed before repair. After cleaning and adjustment, the gap was set to 0.30 mm and the idle-frequency measurement increased to 485 Hz. However, sensor replacement and air-gap correction were implemented together. The present design therefore cannot independently quantify how much of the improvement was attributable to the replacement sensor and how much was attributable to the gap adjustment.

Integrated Diagnostic Interpretation and Relation to Previous Studies

The central contribution of this case is the diagnostic chain created by combining evidence rather than relying on a single reading. OBD-II scanning established the ECU-level symptom pattern; elevated hot and cold resistance indicated an abnormal sensor electrical condition; reduced reported signal amplitude and frequency provided a second electrical indication; and excessive air gap supplied a plausible mechanical contributor. Normalization of these parameters after repair then corroborated the overall diagnosis. This layered logic is consistent with the broader diagnostic principle that fault isolation becomes more credible when independent or partially independent information sources converge (Hu et al., 2018; Mohammadpour et al., 2012). It is better described as multi-method cross-verification than as statistical cross-validation.

The findings complement rather than displace established misfire-detection approaches. Crankshaft-speed and model-based methods can identify cylinder irregularity from rotational dynamics (Geveci et al., 2005; Jung et al., 2015; Kiencke, 1999; Osburn et al., 2006; Tinaut et al., 2007; Wang & Chu, 2005), while vibration and acoustic methods provide alternative mechanical signatures of abnormal combustion (Chang et al., 2002; Delvecchio et al., 2018; Firmino et al., 2021; Jafarian et al., 2018; Sharma et al., 2014). Data-driven and simulation-assisted approaches can add automated classification and robustness under richer datasets or more complex operating conditions (Chen & Randall, 2015; Liu et al., 2013; Qin et al., 2021; Wang et al., 2020; Zheng et al., 2019). The present case extends this literature at the application level by showing how low-cost workshop measurements can be sequenced transparently when symptoms are already pronounced and instrumentation is limited.

The faulty-to-post-repair comparison also illustrates why diagnostic claims should be calibrated to the structure of the intervention. Several abnormal indicators moved toward the reference condition after repair: DTCs cleared, idle speed stabilized, STFT decreased, coil resistance fell within the operational range, the reported signal amplitude and frequency increased, and the air gap returned to 0.30 mm. Taken together, this pattern is strong corroborative evidence that the CKP subsystem was central to the observed problem. It is not, however, a controlled component-isolation experiment because the sensor replacement and mechanical gap correction occurred in the same repair episode. The revised interpretation therefore separates what was observed directly from what is inferred from the converging measurements.

Vocational Education Contribution

The educational value of the procedure lies in its structure as an evidence-based troubleshooting sequence. Competence-based vocational education emphasizes integration of knowledge, practical performance, and workplace connectivity rather than isolated procedural recall (Misbah et al., 2020; Wesselink et al., 2010). In an automotive vocational setting, the four diagnostic stages can therefore be mapped to competencies such as interpreting DTCs and live data, measuring electrical resistance safely, relating signal values to sensor operation, measuring mechanical clearance, comparing observations with reference specifications, and justifying a repair decision from converging evidence. These activities are also compatible with the broader emphasis on problem solving and domain-general competencies in technical vocational learning environments (Löfgren et al., 2023; Schauer et al., 2025). Nevertheless, no students, teachers, learning outcomes, competency scores, or instructional interventions were evaluated in this study; the educational contribution is therefore a proposed application framework, not an empirically validated pedagogical model.

For competency-based use, the sequence can be organized as a diagnostic performance task: learners first formulate a fault hypothesis from symptoms and DTCs; second, select and safely operate an appropriate measuring instrument; third, compare measurements with documented reference values; fourth, connect electrical and mechanical evidence to an engine-management explanation; and fifth, justify a repair and verify the outcome through a post-repair retest. Such an activity could assess procedural accuracy, evidence interpretation, diagnostic reasoning, and documentation quality. The proposed use reflects the connectivity between school-based and workplace-oriented competence development described in vocational education research (Misbah et al., 2020; Wesselink et al., 2010), but its learning effects remain to be tested directly.

Limitations, Transferability, and Practical Implications

Several limitations define the boundary of the findings. First, the evidence is derived from one Daihatsu Xenia 1.0 non-VVT-i with an EJ-DE engine and a passive magnetic pickup CKP sensor. Second, the service-manual source for the numerical diagnostic thresholds was not included in the source manuscript, so those values are reported as operational reference specifications. Third, the make/model and rated accuracy of the multimeter and caliper were not recorded, and individual repeated measurements were unavailable for variability analysis. Fourth, waveform morphology cannot be assessed because no oscilloscope was documented. Fifth, the repair combined sensor replacement and air-gap adjustment, preventing independent attribution of the outcome to either intervention. The general diagnostic logic—cross-checking ECU data, sensor resistance, signal behavior, and mechanical spacing—may be transferable to other passive inductive CKP systems, but numerical thresholds, ECU responses, firing-order effects, and cylinder-specific symptoms remain vehicle- and system-dependent. Future studies should use staged interventions, fully specified instrumentation, retained replicate data, service-manual citations, multiple vehicles and CKP architectures, and direct evaluation with learner groups if educational effectiveness is claimed.

From a workshop-governance perspective, the revised procedure also emphasizes documentation discipline. Each diagnostic stage should record the operating condition, instrument used, reference value, observed value, interpretation, and decision to proceed to the next test. This is especially important when a diagnosis depends on several moderately informative observations rather than one definitive measurement. In future replications, retaining all repeated readings would allow calculation of within-condition variability and would make it possible to distinguish stable deviations from measurement noise. Recording the exact replacement sensor specification, ambient temperature, battery condition, and authoritative service-manual reference would further strengthen traceability. A staged repair design—first correcting the air gap while retaining the original sensor, then replacing the sensor only if the abnormality persists—would provide a clearer estimate of the independent contribution of mechanical spacing and sensor-coil condition. These additions would convert the present diagnostic case into a more reproducible engineering protocol while preserving the practical, low-cost character that makes the approach relevant to routine workshops and vocational laboratories.

CONCLUSION

In this single-vehicle EJ-DE case, asymmetric ignition symptoms in cylinders 2 and 3 were accompanied by P0335/P0336 DTCs, low and unstable idle speed, elevated STFT, CKP resistance above the operational reference range, reduced reported CKP signal amplitude and frequency, and an excessive 0.58 mm air gap. After CKP sensor replacement and air-gap adjustment to 0.30 mm, the measured parameters returned to the reported reference ranges and no active CKP DTC remained after retesting. The combined electrical, OBD-II, and mechanical evidence therefore corroborates a CKP-related diagnosis in this specific vehicle, while the combined repair prevents independent causal attribution to sensor-coil degradation or air-gap deviation alone. The multi-method sequence offers a practical framework for evidence-based workshop troubleshooting and may be adapted for competency-oriented automotive vocational training, but transferability across vehicles and instructional effectiveness should be validated in future research.

REFERENCES

Canal, R., Riffel, F. K., & Gracioli, G. (2024). Machine learning for real-time fuel consumption prediction and driving profile classification based on ECU data. *IEEE Access*, *12*, 68586-68600. https://doi.org/10.1109/ACCESS.2024.3400933

Chang, J., Kim, M., & Min, K. (2002). Detection of misfire and knock in spark ignition engines by wavelet transform of engine block vibration signals. *Measurement Science and Technology*, *13*(7), 1108-1114. https://doi.org/10.1088/0957-0233/13/7/319

Chen, J., & Randall, R. B. (2015). Improved automated diagnosis of misfire in internal combustion engines based on simulation models. *Mechanical Systems and Signal Processing*, *64-65*, 58-83. https://doi.org/10.1016/j.ymssp.2015.02.027

Delvecchio, S., Bonfiglio, P., & Pompoli, F. (2018). Vibro-acoustic condition monitoring of internal combustion engines: A critical review of existing techniques. *Mechanical Systems and Signal Processing*, *99*, 661-683. https://doi.org/10.1016/j.ymssp.2017.06.033

Devasenapati, S. B., Sugumaran, V., & Ramachandran, K. I. (2010). Misfire identification in a four-stroke four-cylinder petrol engine using decision tree. *Expert Systems with Applications*, *37*(3), 2150-2160. https://doi.org/10.1016/j.eswa.2009.07.061

Firmino, J. L., Neto, J. M., Oliveira, A. G., Silva, J. C., Mishina, K. V., & Rodrigues, M. C. (2021). Misfire detection of an internal combustion engine based on vibration and acoustic analysis. *Journal of the Brazilian Society of Mechanical Sciences and Engineering*, *43*(7), 336. https://doi.org/10.1007/s40430-021-03052-y

Geveci, M., Osburn, A. W., & Franchek, M. A. (2005). An investigation of crankshaft oscillations for cylinder health diagnostics. *Mechanical Systems and Signal Processing*, *19*(5), 1107-1134. https://doi.org/10.1016/j.ymssp.2004.06.009

Hmida, A., Hammami, A., Chaari, F., Ben Amar, M., & Haddar, M. (2021). Effects of misfire on the dynamic behavior of gasoline engine crankshafts. *Engineering Failure Analysis*, *121*, 105149. https://doi.org/10.1016/j.engfailanal.2020.105149

Hu, J., Huang, T., Zhou, J., & Zeng, J. (2018). Electronic systems diagnosis fault in gasoline engines based on multi-information fusion. *Sensors*, *18*(9), 2917. https://doi.org/10.3390/s18092917

Huang, T., Pan, H., & Sun, W. (2023). A sensor fault detection, isolation, and estimation method for intelligent vehicles. *Control Engineering Practice*, *139*, 105620. https://doi.org/10.1016/j.conengprac.2023.105620

Ilkivová, M. R., Rohal'-Ilkiv, B., & Neuschl, T. (2002). Comparison of a linear and nonlinear approach to engine misfires detection. *Control Engineering Practice*, *10*(10), 1141-1146. https://doi.org/10.1016/S0967-0661(02)00080-1

Jafarian, K., Mobin, M., Jafari-Marandi, R., & Rabiei, E. (2018). Misfire and valve clearance faults detection in the combustion engines based on a multi-sensor vibration signal monitoring. *Measurement*, *128*, 527-536. https://doi.org/10.1016/j.measurement.2018.04.062

Jung, D. E., Eriksson, L., Frisk, E., & Krysander, M. (2015). Development of misfire detection algorithm using quantitative FDI performance analysis. *Control Engineering Practice*, *34*, 49-60. https://doi.org/10.1016/j.conengprac.2014.10.001

Kiencke, U. (1999). Engine misfire detection. *Control Engineering Practice*, *7*(2), 203-208. https://doi.org/10.1016/S0967-0661(98)00150-6

Liu, B., Zhao, C., Zhang, F., Cui, T., & Su, J. (2013). Misfire detection of a turbocharged diesel engine by using artificial neural networks. *Applied Thermal Engineering*, *55*(1-2), 26-32. https://doi.org/10.1016/j.applthermaleng.2013.02.032

Löfgren, S., Ilomäki, L., Lipsanen, J., & Toom, A. (2023). How does the learning environment support vocational student learning of domain-general competencies? *Vocations and Learning*, *16*(2), 343-369. https://doi.org/10.1007/s12186-023-09318-x

Macián, V., Luján, J. M., Guardiola, C., & Perles, A. (2006). A comparison of different methods for fuel delivery unevenness detection in diesel engines. *Mechanical Systems and Signal Processing*, *20*(8), 2219-2231. https://doi.org/10.1016/j.ymssp.2005.04.001

Misbah, Z., Gulikers, J., Dharma, S., & Mulder, M. (2020). Evaluating competence-based vocational education in Indonesia. *Journal of Vocational Education & Training*, *72*(4), 488-515. https://doi.org/10.1080/13636820.2019.1635634

Mohammadpour, J., Franchek, M., & Grigoriadis, K. (2012). A survey on diagnostic methods for automotive engines. *International Journal of Engine Research*, *13*(1), 41-64. https://doi.org/10.1177/1468087411422851

Osburn, A. W., Kostek, T. M., & Franchek, M. A. (2006). Residual generation and statistical pattern recognition for engine misfire diagnostics. *Mechanical Systems and Signal Processing*, *20*(8), 2232-2258. https://doi.org/10.1016/j.ymssp.2005.06.002

Petrov, R., Leontiev, V., Sokolov, O., Bichurin, M., Bozhkov, S., Milenov, I., & Bozhkov, P. (2020). A magnetoelectric automotive crankshaft position sensor. *Sensors*, *20*(19), 5494. https://doi.org/10.3390/s20195494

Qin, C., Jin, Y., Tao, J., Xiao, D., Yu, H., Liu, C., Shi, G., Lei, J., & Liu, C. (2021). DTCNNMI: A deep twin convolutional neural networks with multi-domain inputs for strongly noisy diesel engine misfire detection. *Measurement*, *180*, 109548. https://doi.org/10.1016/j.measurement.2021.109548

Schauer, J., Abele, S., & Etzel, J. M. (2025). Differential development of professional knowledge and problem-solving skills during VET: The role of cognitive resources, school-leaving certificates, and sociodemographic background. *Vocations and Learning, 18,* Article 12. https://doi.org/10.1007/s12186-025-09367-4

Sharma, A., Sugumaran, V., & Devasenapati, S. B. (2014). Misfire detection in an IC engine using vibration signal and decision tree algorithms. *Measurement*, *50,* 370-380. https://doi.org/10.1016/j.measurement.2014.01.018

Theissler, A., Pérez-Velázquez, J., Kettelgerdes, M., & Elger, G. (2021). Predictive maintenance enabled by machine learning: Use cases and challenges in the automotive industry. *Reliability Engineering & System Safety*, *215*, 107864. https://doi.org/10.1016/j.ress.2021.107864

Tinaut, F. V., Melgar, A., Laget, H., & Domínguez, J. I. (2007). Misfire and compression fault detection through the energy model. *Mechanical Systems and Signal Processing*, *21*(3), 1521-1535. https://doi.org/10.1016/j.ymssp.2006.05.006

Trapani, N., & Longo, L. (2023). Fault detection and diagnosis methods for sensors systems: A scientific literature review. *IFAC-PapersOnLine*, *56*(2), 1253-1263. https://doi.org/10.1016/j.ifacol.2023.10.1749

Wang, Y. S., Liu, N. N., Guo, H., & Wang, X. L. (2020). An engine-fault-diagnosis system based on sound intensity analysis and wavelet packet pre-processing neural network. *Engineering Applications of Artificial Intelligence*, *94*, 103765. https://doi.org/10.1016/j.engappai.2020.103765

Wang, Y., & Chu, F. (2005). Real-time misfire detection via sliding mode observer. *Mechanical Systems and Signal Processing*, *19*(4), 900-912. https://doi.org/10.1016/j.ymssp.2004.07.004

Wesselink, R., de Jong, C., & Biemans, H. J. A. (2010). Aspects of competence-based education as footholds to improve the connectivity between learning in school and in the workplace. *Vocations and Learning*, *3*(1), 19-38. https://doi.org/10.1007/s12186-009-9027-4

Zheng, T., Zhang, Y., Li, Y., & Shi, L. (2019). Real-time combustion torque estimation and dynamic misfire fault diagnosis in gasoline engine. *Mechanical Systems and Signal Processing*, *126*, 521-535. https://doi.org/10.1016/j.ymssp.2019.02.048